*Journal of Applied Mechanics and Technical Physics, Vol. 50, No. 1, pp. 72–79, 2009*

# EFFECT OF THE MELT FLOW DIRECTION ON THE TREEING PROCESS IN POLYMERIC INSULATION

**V. A. Volokhin, O. S. Gefle, and S. M. Lebedev**

UDC 678:621.315.61

*This paper presents the results of a study of the effect of the residual mechanical stress formed in solid polymers at the stage of production on the initiation and growth of an electrical tree. It is shown that the time to tree initiation and the time to breakdown of polycarbonate samples can be determined from the results of investigation of treeing parameters.*

**Key words:** *residual mechanical stress, melt flow, tree, polarization optical method, isochromatic fringes, partial discharges, breakdown.*

**Introduction.** One of the main factors responsible for the failure of high-voltage polymeric isolation in a strong electric field is the formation of incomplete-breakdown channels (trees) [1–4]. As a rule, such channels occur in local regions with the maximum electric-field intensity, for example, near electrode edges and polymer defects or in the presence of roughness on the electrode surface. The tree formation and growth depend on various factors: the measuring voltage, the electric-field inhomogeneity coefficient, the distance between the electrodes, the initial state of the samples, residual mechanical stresses, etc. [5, 6]. The formation and distribution of residual mechanical stresses in insulation articles is due to the thermal shrinkage of the polymer, the rate of its cooling, the presence of embedded metal parts, the shape of the article, etc. In addition, the performance characteristics of insulation articles can affect not only technological parameters but also polymer processing methods. For example, in the production of articles by pressure die casting, the distribution of the residual mechanical stress influencing treeing can depend greatly on the polymer melt flow direction [7, 8].

The purpose of the present work was to study the effect of the melt flow direction on the space–time characteristics of treeing in polycarbonate in a highly inhomogeneous electric field.

**Experimental Technique.** Samples with a point–plane electrode system were made of polycarbonate by pressure die casting in specially developed die molds. During the production of samples with various melt flow directions (Fig. 1), the technological parameters of processing of polycarbonate (melt temperature, excess pressure, and cooling rate) remained constant and the melt flow direction was varied by changing the arrangement of the molding channels in the die molds. Steel needles with a diameter of 1 mm and a point curvature radius $r = (7.5 \pm 0.5)$ $\mu$m were used as high-voltage electrodes. An aluminum foil 7 $\mu$m thick was glued to the lower surface of the samples to ensure contact to the grounded plate electrode. The distance between the electrodes was $d = (9.3 \pm 0.3)$ mm, and each set of samples contained not less than 20 pieces.

One of the simplest and the most informative methods of determining the internal mechanical stress arising in articles produced from optically transparent polymeric dielectrics after hardening is the polarization optical method [9]. Fringe patterns of residual mechanical stress distribution in samples with various melt flow directions were recorded on the polarization optical setup shown schematically in Fig. 2. A KGM-24/150 halogen tube was used as a white light source. Before the sample was placed in the cell, the planes of polarization of polaroids 2 and 5 were at an angle of 90° to each other, which yielded black-field fringe patterns. Then, the sample studied was placed in the cell. The anisotropy of the optical properties of the polymer dielectrics due to the presence of residual

Research Institute of High-Current Electronics, Tomsk Polytechnical University, Tomsk 634028; polymer@hvd.tsk.ru. Translated from Prikladnaya Mekhanika i Tekhnicheskaya Fizika, Vol. 50, No. 1, pp. 85–94, January–February, 2009. Original article submitted December 5, 2007.

 

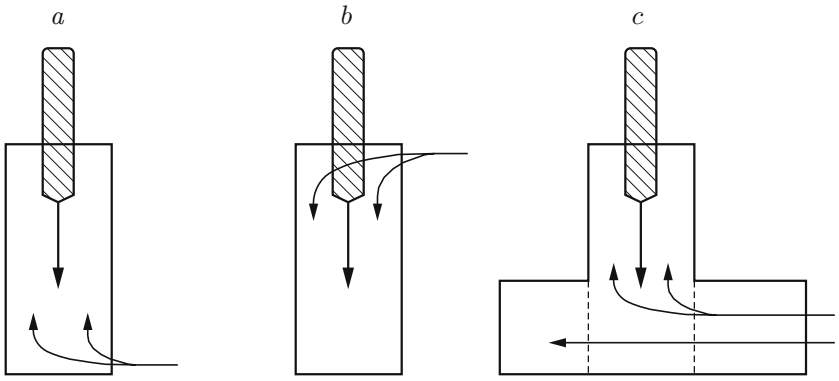


Fig. 1. Diagrams of the production of samples with various melt flow directions: (a) from the plane to the point (mode A); (b) from the point to the plane (mode B); (c) perpendicular to the direction of the electric-field lines (mode C).

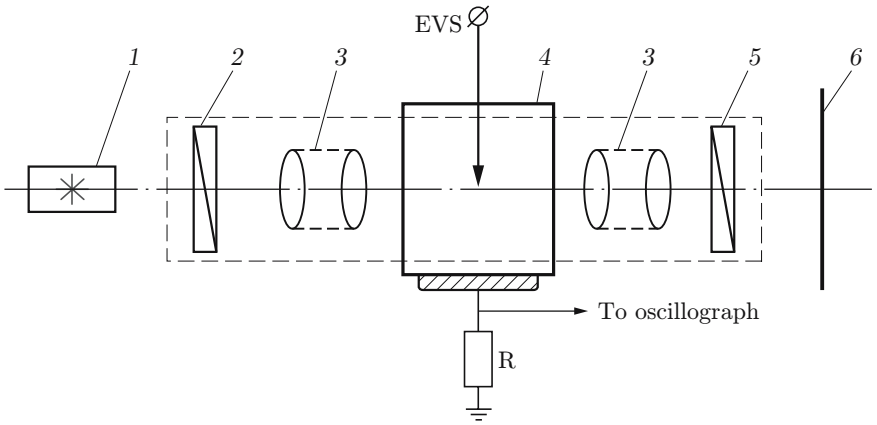


Fig. 2. Diagram of experimental setup: 1) light source; 2) polarizer; 3) system of lenses; 4) sample; 5) analyzer; 6) screen; EVS is the external voltage supply.

internal mechanical stresses led to a significant change in the fringe patterns and to the occurrence of alternating color fringes — isochromatic fringes. The fringe distribution in the samples was recorded by a digital video camera. The spatial resolution of the optical system at the maximum magnification was 25 $\mu$m. For recording and graphical processing of the interference fringes formed near the point during the production of polycarbonate samples, we used a microscope, a digital camera, and a computer. The number and width of fringes of various chromaticity (isochromatic fringes) were determined using the AutoCAD code. The sizes of the fringes were determined by a comparison method with a maximum relative error not exceeding 2%.

The polycarbonate samples were tested at a variable power-frequency voltage of 50 Hz at $U = 24.5$ kV. The voltage was applied to the samples in steps. The maximum intensity of the field at the point was calculated by the formula [10]

$$E = 2U/[r \ln (4d/r)]$$

and for all samples, it was $7.68 \cdot 10^8$ V/m. (Here $U$ [V] is the test voltage, $r$ [m] is the point curvature radius, and $d$ [m] is the distance between the electrodes.)

To study fracture in polycarbonate samples, along with the polarization optical method we employed the partial discharge (PD) method [11] using the traditional procedure for measuring the electric-current pulses arising from ionization processes in the microcracks and hollow tree channels formed in the dielectric under the action of internal mechanical stresses and a strong electric field. When a PD occurs, the external-circuit current causes a voltage drop across the low-induction current shunt R, which is recorded by an oscillograph. The oscillograph was graduated using a calibrator with fixed values of the electric charge: 10, 100, and 1000 pC. For single PD pulses,

TABLE 1

Number and Average Sizes of Fringes near the Point in Polycarbonate Samples with Various Melt Flow Directions

| Mode | $M$ | $\Delta$, $\mu$m | $\Delta_{\text{av}}$, $\mu$m |
|---|---|---|---|
| A | $15 \pm 3$ | $610 \pm 53$ | $40.7 \pm 4.8$ |
| B | $12 \pm 2$ | $428 \pm 32$ | $35.7 \pm 3.4$ |
| C | $14 \pm 3$ | $292 \pm 48$ | $20.9 \pm 1.1$ |

TABLE 2

Space–Time Parameters of the Initial Stage of Fracture of Polycarbonate [$d = (9.3 \pm 0.3)$ mm, $r = (7.5 \pm 0.5)$ $\mu$m, and $U = 24.5$ kV]

| Mode | $\tau_0 \pm \Delta\tau_0$, sec | $q_0 \pm \Delta q_0$, pC | $l_0 \pm \Delta l_0$, $\mu$m | |
|---|---|---|---|---|
| | | | calculation | experiment |
| A | $149.0 \pm 16.5$ | $25.90 \pm 5.24$ | $33.6 \pm 6.8$ | $34.0 \pm 8.0$ |
| B | $189.0 \pm 16.6$ | $18.50 \pm 4.08$ | $24.0 \pm 5.3$ | $25.0 \pm 7.0$ |
| C | $233.0 \pm 23.2$ | $14.72 \pm 3.70$ | $19.1 \pm 4.8$ | $19.7 \pm 5.3$ |

**Note.** The parameters $\tau_0$ and $q_0$ and the calculated value of $l_0$ were recorded by the PD method, and the experimental values of $l_0$ by the optical method.

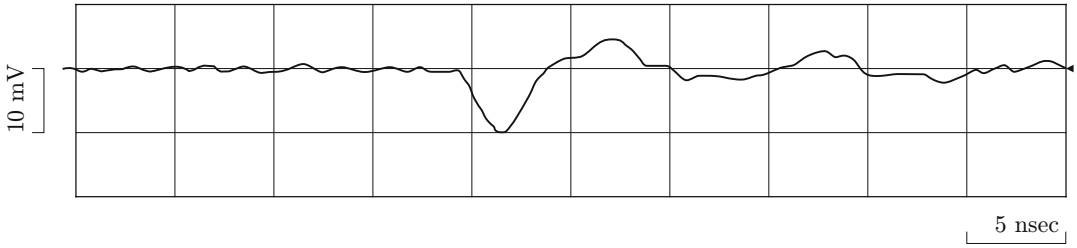


Fig. 3. Primary PD pulse in a polycarbonate sample after crack formation.

the error in measuring the signal amplitude, time intervals, and charge value by an LeCroy oscillograph did not exceed 1.83, 0.86, and 2%, respectively.

After the occurrence and recording of the first PD pulses, the voltage was switched off and the length of primary breakdown channels (microcracks) were measured using a microscope with a measuring sensitivity of 5 $\mu$m. After that, the test of the samples was continued at the same voltage up to their breakdown.

**Experimental Results and Discussion.** An analysis of the fringe patterns has shown that the alternation of the color of isochromatic fringes near the point is almost independent of the melt flow direction at the stage of production of the samples. Near the point, as a rule, a light-pink fringe is followed by a light-green fringe, which is followed by a light-pink fringe again, etc. The melt flow direction affects the number of fringes near the point $M$, the total width of the fringes $\Delta$, and the average size of one fringe $\Delta_{\text{av}}$.

The smallest average values of the total width of the isochromatic fringes were observed for the transverse direction of the melt flow (mode C), and their largest values were observed for the melt flow direction from the plane to the point (mode A) (Table 1). Microscopic observation of all samples in the initial state did not reveal microcracks or microcavities near the point.

In a time interval $\tau_0$ after a sudden increase in the voltage, single PD pulses occurred, whose characteristic shape is shown in Fig. 3. For samples with various melt flow directions, the length of the front of the primary PD pulses with positive or negative polarity was 1.5 to 2.5 nsec, and the length of the pulses was 3 to 5 nsec. The smallest values of the single PD pulse amplitude $U_0$ and the charge $q_0$, characteristic of the onset of the fracture of polycarbonate, were observed for the transverse melt flow direction (Table 2).

As a rule, the spatial resolution of the polarization optical setup is insufficient to record the initial stage of fracture of polycarbonate. Therefore, after the occurrence of the first PD pulses, the voltage was switched-off and the fracture characteristics and the linear sizes of the primary channels (microcracks) were determined under a microscope. A comparison of the primary fracture channels of polycarbonate (microcracks or trees) recorded by

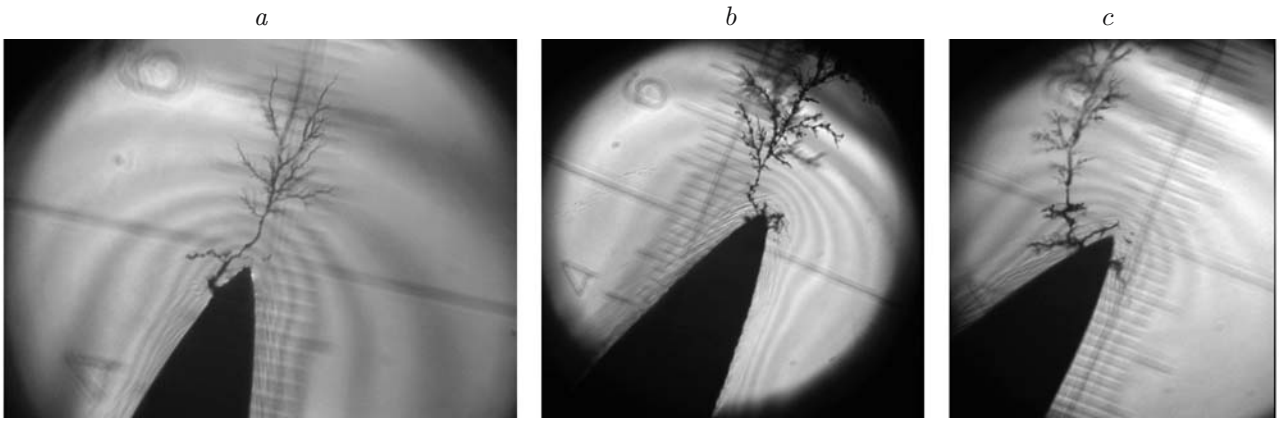


Fig. 4. Tree growth in polycarbonate samples at $t = 750$ (a), 1100 (b), and 7500 sec (c).

the PD method and the optical method shows that the single PD pulse amplitude and the magnitude of the charge $q_0$ are proportional to the channel length $l_0$, which can be calculated by the formula

$$l_0 = q_0/(\sqrt{2}\,U\varepsilon_0 n^2) \tag{1}$$

($q_0$ [C] is the magnitude of the charge of the individual PD pulse recorded at the time $t = \tau_0$, $U$ [V] is the measuring voltage, $\varepsilon_0 = 8.854 \cdot 10^{-12}$ [F/m] is the electrical constant, and $n = 1.585$ is the refractive index for polycarbonate).

The length of the primary channels measured with the aid of a microscope and the values of $l_0$ calculated by formula (1) for $t = \tau_0$ are given in Table 2, from which it follows that the difference between the calculated and experimental values $l_0$ does not exceed 5%.

We note that the value of $l_0$ in (1) is directly proportional to the capacitance of the fractured region of the dielectric $C_0 = q_0/(\sqrt{2}U)$ at the time $t = \tau_0$ and is inversely proportional to the square of the refractive index for polycarbonate at ultrahigh (optical) frequencies. Thus, the single PD pulses recorded at the beginning of the fracture process provide information on the linear sizes of fracture region; in this case, the average width of the isochromatic fringes $\Delta_{\text{av}}$ (see Table 1) and the primary-channel lengths $l_0$ (see Table 2) correlate with each other: the smaller $\Delta_{\text{av}}$, the smaller $l_0$.

During the tests of the samples, it was found that, in the initial stage of fracture of polycarbonate, the parameters of each single pulse PD at the time $t = \tau_i$ characterized the linear sizes of the $i$th microcrack up to tree initiation. At $t = \tau_i$ and $q = q_i$, the value of $l_i$ can be calculated with sufficient accuracy by formula (1) for each sample. In addition, in most of the samples, several rather than one microcracks formed near the point; with time, they merged to form a net of microcracks around the needle. Subsequently, a tree originated from on one of these microcracks (Fig. 4); we denote the treeing time by $\tau_{\text{tr}}$.

In comparison with the PD method, the polarization optical method records the fracture with a delay due to the time required to carburize the walls of microcracks or hollow tree channels during the occurrence of PDs in them. The delay ($\tau_{\text{delay}}$) can vary significantly, depending on the PD intensity; therefore, for $\tau_{\text{delay}} \approx \tau_0$, this method is unsuitable for recording the time intervals characterizing the beginning of the fracture process. For all tested samples, $\tau_{\text{delay}} \geqslant 60$ sec on the average; therefore, as the time of fracture onset, we used the time $\tau_0$ (see Table 2) corresponding to the time of recording of the first PD pulse.

In the time interval $(\tau_0, \tau_{\text{tr}})$, the fracture propagation in time and space had a discrete nature, and microcracks, as a rule, formed within one to three fringes and their total width (within the measurement error) coincided with the experimental and calculated linear sizes of microcracks.

At the moment of treeing in all tested samples, the amplitude of PD pulses increased sharply (on the average by a factor of 5–15) compared to the amplitude of the primary PD pulse (Fig. 5). It was found that the PD pulse amplitude was proportional to the tree channel length until the formation of lateral branches from the main tree channel (see Fig. 4).

In most cases, microchannels formed on the lateral surfaces of the point; therefore, the treeing time was determined not by the maximum field intensity at the point, which was $7.68 \cdot 10^8$ V/m for all tested samples, but

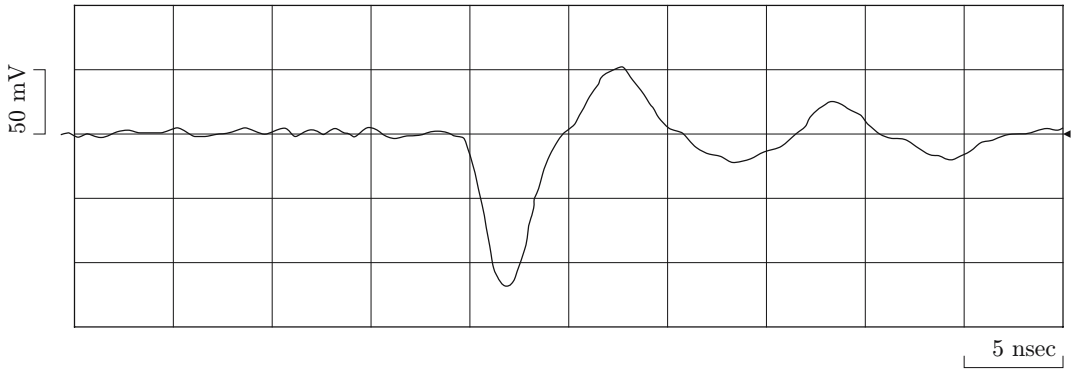


Fig. 5. PD pulse in a polycarbonate sample after tree initiation.

TABLE 3

Space–Time Fracture Parameters of Polycarbonate
[$d = (9.3 \pm 0.3)$ mm, $r = (7.5 \pm 0.5)$ $\mu$m, and $U = 24.5$ kV]

| Mode | $\tau_{\rm tr} \pm \Delta\tau_{\rm tr}$, sec | $l_{\rm tr} \pm \Delta l_{\rm tr}$, $\mu$m | $\tau_{\rm br} \pm \Delta\tau_{\rm br}$, sec |
|---|---|---|---|
| A | $9826 \pm 1319$ | $193 \pm 76$ | $18{,}520 \pm 1736$ |
| B | $13{,}532 \pm 1958$ | $189 \pm 48$ | $21{,}456 \pm 2743$ |
| C | $16{,}725 \pm 3570$ | $165 \pm 39$ | $26{,}303 \pm 3608$ |

by the PD intensity. The formation of primary channels mainly on the lateral surfaces of the point indicates that the time of their formation $\tau_0$ at the same maximum field intensity at the point depends greatly on the value of the residual mechanical stress. Thus, fracture of polycarbonate samples produced by pressure die casting begins with the formation of microcracks under the action of not only the ponderomotive forces arising from the application of an external electric field [12, 13] but also under the action of internal mechanical stresses. Since the time of occurrence of primary PD pulses $\tau_0$ depends greatly on the melt flow direction during sample production (see Table 2), it should also depend on the distribution of the internal mechanical stresses near the point and their spatial orientation. This assumption is supported by the fact that the time of primary-crack formation $\tau_0$ and the time of fracture propagation in the mechanically stressed region depend on the width and number of fringes: the smaller the width of the fringes and the larger their number, the larger the value of $\tau_0$ and the treeing time $\tau_{\rm tr}$. In other words, the boundaries between the fringes are barriers to the growing microcracks, leading to a change in their propagation direction and a retardation of their growth (see Fig. 4).

Table 3 gives experimental space–time fracture parameters of polycarbonate samples with various melt flow directions determined by the polarization optical method. The maximum values of $\tau_{\rm tr}$ and the time to breakdown $\tau_{\rm br}$ are observed for polycarbonate samples with the transverse melt flow direction (mode C), which are characterized by the least width of the isochromatic fringes (see Table 1) and microcrack formation predominantly in the transverse direction.

From the results of a correlation analysis of the time parameters of polycarbonate fracture obtained by the polarization optical method and the PD method, it follows that in samples with various melt flow directions, the treeing time $\tau_{\rm tr}$ and the time to breakdown $\tau_{\rm br}$ can be estimated by the formulas

$$\tau_{\rm tr} = \tau_0 \sqrt{|\varepsilon^*_\infty|}\, \exp|\varepsilon^*_\infty|, \qquad \tau_{\rm br} = \tau_{\rm tr} \sqrt{|\varepsilon^*_\infty|}, \tag{2}$$

where $|\varepsilon^*_\infty| = \sqrt{2}\, n^2 = \sqrt{2}\, \varepsilon_\infty$ is the modulus of the complex dielectric permeability at ultrahigh optical frequencies provided that its real component $\varepsilon'_\infty$ is equal to the imaginary component $\varepsilon''_\infty = \varepsilon'_\infty \tan\delta$.

Table 4 gives calculated space–time parameters of polycarbonate fracture obtained from the results of measurement of $\tau_0$ (see Table 2) and $q_{\rm tr}$ ($q_{\rm tr}$ is the average magnitude of the PD pulse charge for $t = \tau_{\rm tr}$). The tree length $l_{\rm tr}$ was calculated by formula (1) for $q = q_{\rm tr}$.

A comparison of the experimental and calculated results given in Tables 3 and 4 shows that the difference in the average values of the parameters does not exceed 10%; in this case, the best agreement between the experimental and calculated data is observed for calculations of $\tau_{\rm tr}$ and $\tau_{\rm br}$ using the experimentally determined values for each

TABLE 4

Space–Time Parameters of Polycarbonate Fracture Recorded by PD

| Mode | $q_{\rm tr} \pm \Delta q_{\rm tr}$, pC | $l_{\rm tr} \pm \Delta l_{\rm tr}$, $\mu$m | $\tau_{\rm tr} \pm \Delta \tau_{\rm tr}$, sec | $\tau_{\rm br} \pm \Delta \tau_{\rm br}$, sec |
|---|---|---|---|---|
| A | $162.5 \pm 53.5$ | $210.8 \pm 69.4$ | $9805 \pm 1086$ | $18{,}481 \pm 2046$ |
| B | $141.4 \pm 35.7$ | $183.5 \pm 46.3$ | $12{,}437 \pm 1093$ | $23{,}443 \pm 2059$ |
| C | $130.0 \pm 29.8$ | $168.7 \pm 38.7$ | $15{,}333 \pm 2178$ | $28{,}900 \pm 4106$ |

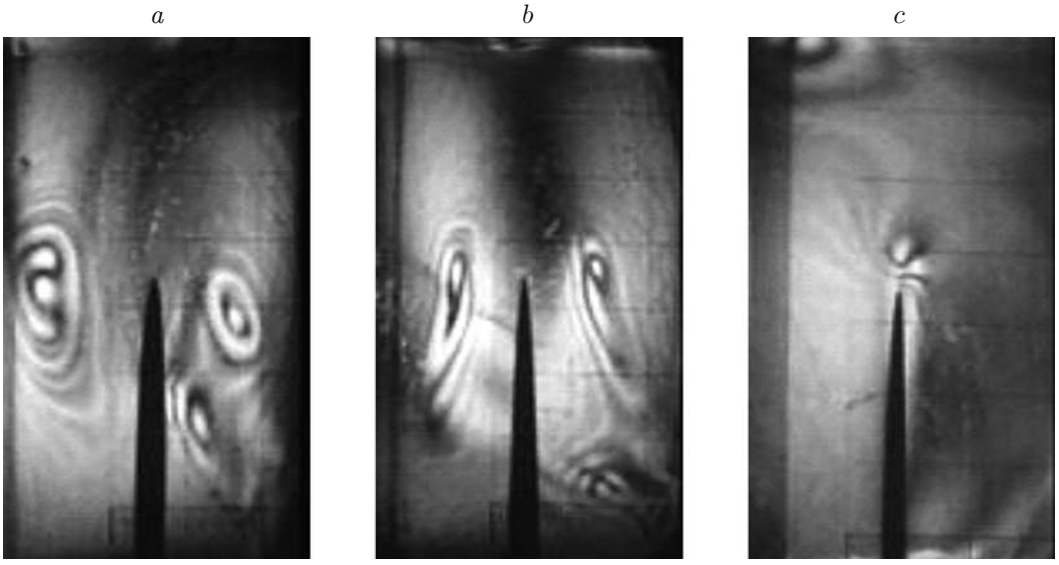


Fig. 6. Typical fringe patterns for samples with various melt flow directions: mode A (a), mode B (b), and mode C (c).

sample. Since in (2), the variable parameter is $\tau_0$, it is obvious that time of tree initiation and the time to breakdown of the sample depend on the initial conditions of primary-crack formation. For the transverse melt flow direction (mode C), the average value of $\tau_0$ is 56 and 23% larger than that for modes A and B, respectively, which results in increased durations of the treeing stage and the stage preceding the breakdown of the sample.

From (2), it also follows that the time of tree growth is proportional to the complex refractive index, and the time of formation of incomplete-breakdown channels is proportional to the modulus of the complex dielectric permeability. It should be noted that breakdown of a local site of the dielectric occurs when the real and imaginary parts of the complex dielectric permeability become equal: $\varepsilon' = \varepsilon''$. The same condition for breakdown of polymer dielectrics was obtained earlier for both homogeneous and highly inhomogeneous external electric fields [14, 15].

The results of the studies show that the fracture process can be controlled by varying the melt flow direction. Figure 6 shows typical fringe patterns in samples with various melt flow directions. It is evident that in the case of mode C, the reflected melt flows form a fringe pattern that differ significantly from the corresponding patterns for the longitudinal melt flow direction (modes A and B).

Usually, the trees formed in the samples produced in modes A and B have a weakly branched shape and develop predominantly along the axis of the interelectrode gap (Fig. 7a). In samples with the transverse melt flow direction, branched trees are formed, as a rule, and the growing tree channels are focused mostly along the boundaries between neighboring isochromatic fringes (Fig. 7b). The curvature of the channels and the departure of their trajectory from the direction of the electric-field lines leads to an increase in the fracture propagation time and the time to breakdown $\tau_{\rm br}$, and, in the presence of vortex flows on the path of formation of the main breakdown channel, this leads to the arrival of the channel at the lateral surface of the sample (Fig. 7c).

**Conclusion.** An analysis of the results of the study leads to the following conclusions.

In polycarbonate samples produced by pressure die casting, fracture begins with the formation of microcracks mainly on the lateral surfaces of the point and is accompanied by the occurrence of single PD pulses with the front and pulse lengths not more than 2.5 and 5 nsec, respectively.

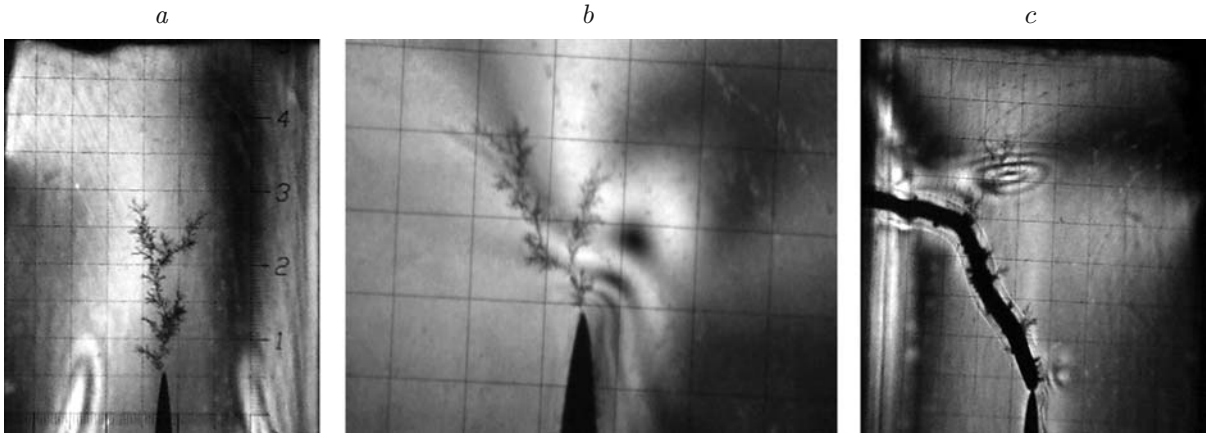


Fig. 7. Effect of melt flow direction on the shape and spatial orientation of tree channels: (a) longitudinal melt flow direction; (b) transverse melt flow direction; (c) curvature of the breakdown channel in the presence of vortex flow near the plate electrode.

In the initial stage of fracture, the magnitude of the single PD pulse charge is proportional to the length of the microcrack or tree, which allows the linear sizes of the fracture region to be estimated with a relative error not exceeding 5%.

The linear sizes of microcracks correlate with the interference fringe width dependent on the melt flow direction. The average length of primary microcracks is 76% smaller for the transverse than for the longitudinal melt flow direction from the plane to the point.

The time of formation of a primary crack and the time of fracture propagation in the mechanically stressed region depend on the width and number of fringes, i.e., on the spatial distribution of the mechanical stress. For the transverse melt flow direction, the time of primary-crack formation is 23–56% larger than for the longitudinal melt flow direction.

The boundaries of the fringes are barriers to the growing cracks or incomplete-breakdown channels, leading to a curvature of their trajectory, an increase in the treeing time and the time to breakdown of the samples.

The time of tree initiation and the time of breakdown of the clearance depend on the time of primary-crack formation, the complex refractive index, and the modulus of the complex dielectric permeability at optical frequencies, which allows the time parameters of polycarbonate fracture to be predicted with a relative error not exceeding 10%.

## REFERENCES

1. Y. Shibuya, S. Zoledziowski, and J. Calderwood, "Void formation and electrical breakdown in epoxy resin," *IEEE Trans. Power Appar. Syst.*, **96**, 198–206 (1977).
2. O. S. Gefle, "Development of a method for diagnosing the initiation and development of fracture in electrical insulation using thermal effects," Candidate Dissertation in Tech. Sci., Tomsk (1984).
3. T. Tanaka and A. Greenwood, "Effect of charge injection and extraction on tree initiation in polyethylene," *IEEE Trans. Power Appar. Syst.*, **97**, 1749–1757 (1978).
4. N. Shimizu and C. Laurent, "Electrical tree initiation," *IEEE Trans. Dielectrics Electric. Insul.*, **5**, 651–659 (1998).
5. O. S. Gefle, "Estimating the integral temperature gradient in the initial stage of fracture of polymeric dielectrics in a strong electric field," *Élektrichestvo*, No. 6, 84–88 (1988).
6. O. S. Gefle, S. M. Lebedev, and Yu. P. Pokholkov, *Barrier Effect in Dielectrics* [in Russian], TML-press, Tomsk (2007).
7. S. M. Lebedev, O. S. Lebedev, V. A. Volokhin, and P. V. Volokhin, "Effect of a melt flow direction on the treeing process in polymeric dielectrics," in: *Proc. of the 15th Int. Symp. on High Voltage Eng.*, Ljubljana, August 27–31 (2007), Paper No. 476.

8. O. S. Gefle, S. M. Lebedev, V. A. Volokhin, and Y. P. Pokholkov, "Effect of the mechanical strain on the treeing phenomenon," in: *Proc. of the Int. Conf. on Solid Dielectrics*, Winchester, July 8–13 (2007), pp. 142–145.
9. A. Ya. Aleksandrov and M. Kh. Akhmetzyanov, *Polarization Optical Methods in Deformable Solid Mechanics* [in Russian], Nauka, Moscow (1973).
10. J. H. Mason, "Breakdown of solid dielectrics in divergent fields," *Proc. IEE.*, **102**, 254–263 (1955).
11. G. S. Kuchinskii, *Partial Discharges in High-Voltage Constructions* [in Russian], Énergiya, Leningrad (1979).
12. D. W. Auckland, A. A. McNicol, and B. R. Varlow, "Development of strain in solid dielectric due to vibrational electrostatic forces," *J. Phys., D: Appl. Phys.*, **23**, 1608–1613 (1990).
13. B. R. Varlow and D. W. Auckland "The influence of mechanical factors on electrical treeing," *IEEE Trans. Dielectrics Electric. Insul.*, **5**, 761–766 (1998).
14. O. S. Gefle, "Critical parameters of imperfect dielectrics in strong electric field," in: *Proc. of the 9th Int. Symp. on High Voltage Eng.*, Graz (1995), Paper No. 1069.
15. S. A. Boggs, "Theory of a defect-tolerant dielectric system," *IEEE Trans. Electric. Insul.*, **28**, 365–370 (1993).